

# Depth-dependent crystallinity of nano-crystalline silicon induced by step-wise variation of hydrogen dilution during hot-wire CVD

C J Arendse<sup>1</sup>, B A van Heerden<sup>1</sup>, T F G Muller<sup>1</sup>, F R Cummings<sup>1</sup>, C J Oliphant<sup>2</sup>, G F Malgas<sup>1</sup> and D E Motaung<sup>3</sup>

<sup>1</sup> Department of Physics, University of the Western Cape, Private Bag X17, Bellville 7535, South Africa

<sup>2</sup> National Metrology Institute of South Africa, Private Bag X34, Lynnwood Ridge, Pretoria 0004, South Africa

<sup>3</sup> DST/CSIR National Centre for Nano-Structured Materials, P. O. Box 395, Pretoria 0001, South Africa

E-mail: carendse@uwc.ac.za

**Abstract.** To induce an amorphous surface in a nano-crystalline silicon (nc-Si:H) thin film, the hydrogen dilution was reduced step-wise at fixed time intervals from 90 – 50% during the hot-wire chemical vapour deposition process. This contribution reports on the structural properties of the resultant nc-Si:H thin film as a function of the deposition time. Raman spectroscopy, confirmed by high resolution transmission spectroscopy, indicates crystalline uniformity in the growth direction, accompanied by the progression of an amorphous surface layer as the deposition time is increased. The silicon- and oxygen bonding configurations were probed using infrared spectroscopy and electron energy loss spectroscopy. The growth mechanism is ascribed to the improved etching rate by atomic hydrogen in nano-crystalline silicon towards the film/substrate interface region. The optical properties were calculated by applying the effective medium approximation theory, where the existence of bulk and interfacial layers, as inferred from cross-sectional microscopy, were taken into account.

## 1. Introduction

The use of hydrogenated nano-crystalline silicon (nc-Si:H) thin films as the absorber intrinsic layer in silicon thin film solar cells has been extensively investigated, mainly due its improved photo-induced stability [1-2]. The hot-wire chemical vapour deposition (HWCVD) technique, based on the catalytic decomposition of the SiH<sub>4</sub> and H<sub>2</sub> gas by a heated transition metal filament, has been established as a viable deposition technique for nc-Si:H [3]. The structural and opto-electronic properties of the thin films are dependent on the deposition parameters, of which the hydrogen (H) dilution and substrate temperature are the most crucial. It has been reported that the best nc-Si:H based solar cells, with optimal opto-electronic properties, are deposited near to the amorphous/nano-crystalline silicon transition regime [4]. It is well known that nc-Si:H has a distinct structural inhomogeneity in the growth direction, which initiates with an amorphous incubation layer that transitions into an increased crystallite size and fraction as the growth progresses. This non-uniformity in the crystallinity with thickness results in the formation of cracks within the thin films and a reduced short-circuit current in solar cells, which eventually leads to deterioration in the solar cell performance [5]. The hydrogen



profiling technique, where the hydrogen dilution is continuously decreased as a function of deposition time, has been proposed to maintain a fixed crystallite size and fraction as a function of depth [6-7]. In this contribution, we propose a HWCVD hydrogen profiling sequence where the H dilution ratio is changed from 90 to 50% at fixed time intervals to enable an investigation into the evolution of the structural properties as a function of deposition time and the eventual optical properties.

## 2. Experimental

The nc-Si:H thin films were deposited by HWCVD, using mixtures of SiH<sub>4</sub> and H<sub>2</sub> gas, decomposed over a tantalum filament heated to 1600 °C. A detailed description of the experimental set-up is given elsewhere [8]. With the exception of the H dilution ratio  $R$  (defined as ratio of the flow rate of H<sub>2</sub> to the total gas flow rate), the substrate temperature, total gas flow rate and deposition pressure were fixed at 240 °C, 30 sccm and 60  $\mu$ bar, respectively. The film series were deposited sequentially at  $R = 90\%$ , 83%, 80% and 50% for 900 s, 720s, 480 s and 300 s, respectively.

Fourier transform infrared (FTIR) absorption spectra were collected in transmission geometry from 400 – 4000 cm<sup>-1</sup> with a spectral resolution of 1 cm<sup>-1</sup>, using a Perkin-Elmer Spectrum 100 FTIR spectrophotometer. The structural properties were investigated using a Horiba Jobin-Yvon T64000 micro-Raman spectrometer in backscattering geometry at room temperature. The Raman spectra were collected in the region 100 – 1000 cm<sup>-1</sup> with a spectral resolution of 0.4 cm<sup>-1</sup>, using excitation wavelengths of 532 and 647 nm. A cross-section of the final thin film was prepared by a FEI Helios NanoLab 650 Dual Beam focussed-ion beam SEM (FIBSEM), which were subsequently analysed in a FEI Tecnai F20 FEGTEM in bright field mode at an accelerating voltage of 200 kV. Electron energy loss spectroscopy (EELS) spectra were collected using a Gatan Image Filter (GIF2001) at an energy dispersion of 5eV/channel and resolution of 1.3 eV. Optical transmission spectra were measured using a CARY 1E UV/VIS spectrometer in the range 200 – 900 nm with a spectral resolution of 1 nm. Raman and FTIR spectra were collected on the films deposited after each time interval (900 s, 1620 s, 2100 s and 2400 s), whereas TEM, EELS and UV/VIS spectroscopy were performed only on the final thin film (2400 s).

## 3. Results and Discussion

The Raman spectra of the sample series at different thicknesses, using an excitation wavelength of 532 nm, are given in figure 1. The film thickness was extracted by interferometry from the UV/VIS transmission spectra. The initial thin film deposited at  $R = 90\%$  reveal a distinct crystalline signature, as indicated by the narrow c-Si transverse-optic (TO) peak at 515 cm<sup>-1</sup>. The crystalline fraction of this thin film amounts to 38%. A further growth in the thickness, accompanied by a reduction in  $R$ , results in a large reduction in the intensity of the c-Si TO peak, which eventually disappears. As the Raman signal produced by the excitation wavelength of 532 nm is dominated by the surface of the nc-Si:H thin films, it is evident that the crystalline fraction at the surface decreases with a growth in the film thickness, eventually leading to a breakdown in nc-Si:H growth. The width of the amorphous silicon (a-Si) TO peak at 480 cm<sup>-1</sup> for the final thin film (933 nm-thick) amounts to 53 cm<sup>-1</sup>, which denotes a highly ordered, dense a-Si surface layer [9]. To probe deeper into the thin films, an excitation wavelength of 647 nm was used, for which the Raman spectra are given in figure 2. Analysis of the Raman spectra reveals that the crystalline fraction remains relatively constant at ~ 30% as the film thickness increases, indicative of crystalline uniformity in the growth direction.

FTIR spectroscopy is the technique of choice to probe into the Si, H and O bonding configuration in nc-Si:H. Figure 3 shows the absorption spectra of the stretching vibrations for the sample series at different thicknesses. The mode centred around 2000 cm<sup>-1</sup> is assigned to the Si-H monohydrides in the compact isolated phase of nc-Si:H, whereas the shoulder peak at 2100 cm<sup>-1</sup> is attributed to the Si-H<sub>2</sub>

bonds in the clustered phase, associated with the presence of microvoids. In the initial growth step, H is bonded preferentially in the clustered phase, which signifies a void-rich layer. As the growth progresses, the H content bonded in the compact, isolated phase increases and is accompanied with a reduction of that in the clustered phase. Therefore, as the growth progresses the micro-structure and compactness of the nc-Si:H thin film improves, thereby resulting in a more dense and stable thin film. This observation is confirmed by the reduction in oxidation, as inferred from the disappearance of Si-O-Si vibration at around  $1070\text{ cm}^{-1}$  (not shown).

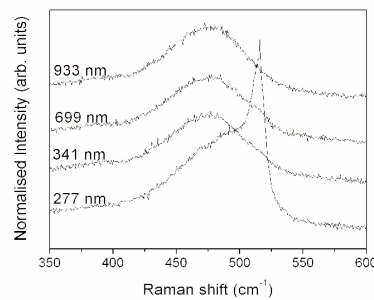


**Figure 1.** Raman spectra using 532 nm excitation.

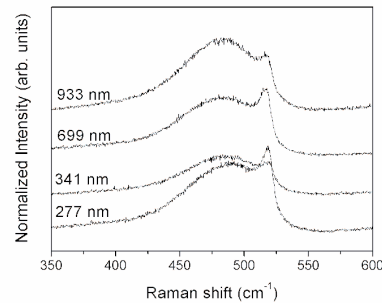


**Figure 2.** Raman spectra using 647 nm excitation.

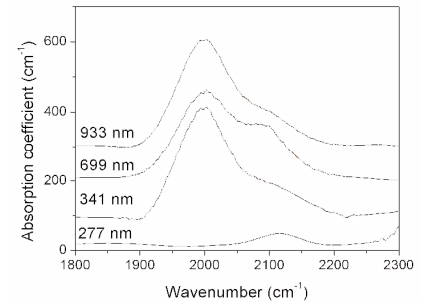


**Figure 3.** FTIR spectra of sample series.

Raman and infrared spectroscopy therefore suggests that the reduction in the hydrogen dilution as the thin film growth progresses, favours the formation of a compact, homogeneous nano-crystalline structure with a dense, highly ordered amorphous silicon surface. The reduction in the hydrogen dilution during the deposition infers a reduction in the amount of atomic hydrogen available for the etching of strained Si-Si surface bonds, thereby promoting the growth of an amorphous silicon surface layer at low  $R$ -values. Furthermore, the continued expansion of the nc-Si:H region at high  $R$ -values is attributed to the preferred etching by atomic hydrogen in the original crystalline regions.

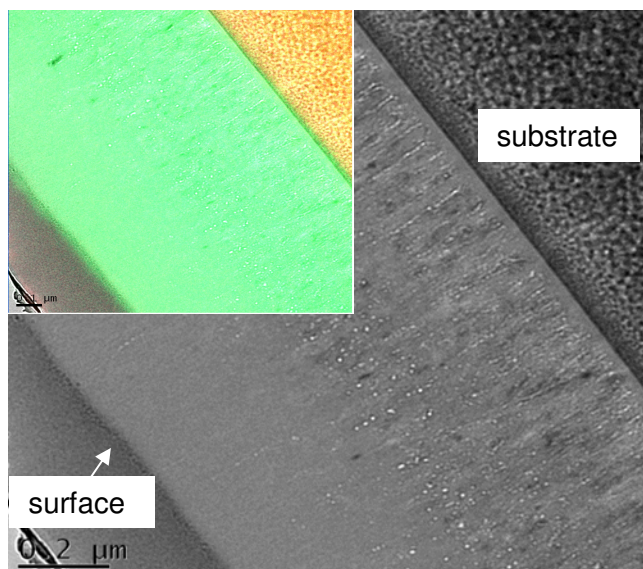


**Figure 4.** TEM micrograph of the final nc-Si:H thin film. Inset shows the overlapping oxygen and silicon EELS maps (Si-green and O-red).

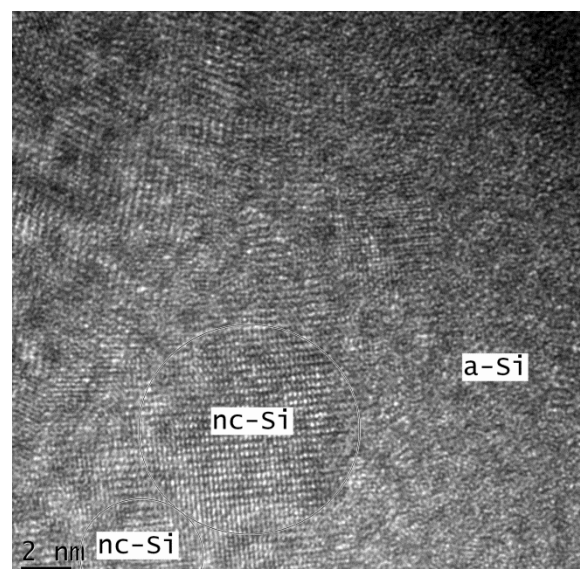


**Figure 5.** HRTEM micrograph showing nc-Si and a-Si regions.

Figure 4 shows the bright field TEM micrograph of the final nc-Si:H thin film, with a thickness of  $\sim 900$  nm, which agrees with the interferometry calculations. A 10 nm-thick amorphous incubation layer is observed at the film/substrate interface, which is characteristic of nc-Si:H grown at high H dilution ratios. Thereafter, a well-defined crystalline region extends 500 nm in the growth direction with a uniform crystalline distribution, which corroborates the Raman analysis. Finally, the thin film is capped with a thick, compact amorphous region. The corresponding overlapping oxygen and silicon EELS maps (inset in Figure 4) shows no detectable oxygen present in the thin film, which confirms the FTIR results. Closer inspection into the crystalline structure by HRTEM reveals distinct nanocrystallites embedded in an a-Si matrix with diameters ranging from 2 to 10 nm (see figure 5).

The optical properties of the final thin film were calculated by applying the effective medium approximation theory, where the existence of all the phases in the bulk and interfacial layers, as inferred from cross-sectional TEM, were taken into account [10]. The refractive index at zero energy ( $n_0$ ) amounts to  $\sim 3.30$ , indicative of a dense nc-Si:H thin film. Regardless of its relatively high crystalline fraction, the absorption coefficient (at 2 eV) amounts to  $2.1 \times 10^4 \text{ cm}^{-1}$ , which is comparable to that of device-quality hydrogenated amorphous silicon.

#### 4. Conclusion

A step-wise decrease in the hydrogen dilution was used to demonstrate the deposition of a structurally improved nc-Si:H/a-Si bilayer structure by hot-wire CVD. Raman spectroscopy, confirmed by TEM, shows the initial formation of a thin a-Si incubation layer at the substrate interface followed by a uniform crystalline structure in the growth direction with a crystalline fraction of 30%. The structure is capped with a dense, highly ordered amorphous silicon layer. The superior density of the thin film is corroborated by the absence of oxidation and the enhanced refractive index.

#### Acknowledgements

The authors acknowledge the financial support of the National Research Foundation. The authors would like to thank the Zernike Institute at Groningen University for the Raman spectroscopy measurements.

#### References

- [1] Meier J, Flückiger R, Keppner H and Shah A 1994 *Appl. Phys. Lett.* **65** 860
- [2] Yan B J, Yue G Z, Banerjee A, Yang J and Guha S 2004 *Mater. Res. Soc. Symp. Proc.* **808** A9.41
- [3] Oliphant C J, Arendse C J, Knoesen D, Muller T F G, Prins S and Malgas G F 2011 *Thin Solid Films* **519** 4437
- [4] van Veen M 2003 *Tandem solar cells deposited using hot-wire chemical vapour deposition* (Utrecht University, The Netherlands)
- [5] Yan B J, Yue G Z, Yang J, Guha S, Williamson D L, Han D X and Jiang C S 2004 *Mater. Res. Soc. Symp. Proc.* **808** A8.5
- [6] Yan B, Yue G, Yang J, Guha S, Williamson D L, Han D and Jiang C S 2004 *Appl. Phys. Lett.* **85** 1955
- [7] Li H, Franken R H, Stolk R L, van der Werf C H M, Rath J K and Schropp R E I 2008 *J. Non-Cryst. Solids* **354** 2087
- [8] Arendse C J, Knoesen D and Britton D T 2006 *Thin Solid Films* **501** 92
- [9] Beeman D, Tsu R and Thorpe M F 1985 *Phys. Rev. B* **32** 874
- [10] Muller T F G, Knoesen D, Arendse C J, Halindintwali S, Malgas G F, Houweling Z S and Schropp R E I 2010 *Phys. Status Solidi C* **7** 750